Article

Reactions of d Group 4 Amides with Dioxygen. Preparation of Unusual Oxo Aminoxy Complexes and Theoretical Studies of Their Formation

Ruitao Wang, Xin-Hao Zhang, Shu-Jian Chen, Xianghua Yu,
Chang-Sheng Wang, David B. Beach, Yun-Dong Wu, and Zi-Ling Xue

J. Am. Chem. Soc., **2005**, 127 (14), 5204-5211• DOI: 10.1021/ja042307u • Publication Date (Web): 24 March 2005

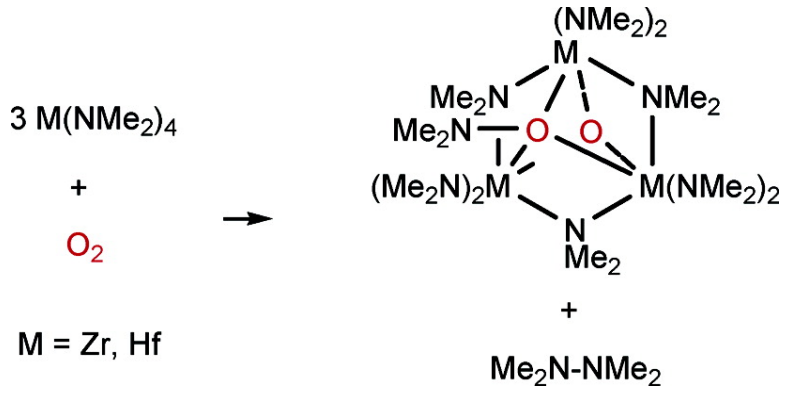

More About This Article

Additional resources and features associated with this article are available within the HTML version:

- Supporting Information
- Links to the 3 articles that cite this article, as of the time of this article download
- Access to high resolution figures
- Links to articles and content related to this article
- Copyright permission to reproduce figures and/or text from this article

View the Full Text HTML

J|A|C|S
ARTICLES
Published on Web 03/24/2005

Reactions of d^0 Group 4 Amides with Dioxygen. Preparation of Unusual Oxo Aminoxy Complexes and Theoretical Studies of Their Formation

Ruitao Wang,[†] Xin-Hao Zhang,[‡] Shu-Jian Chen,[†] Xianghua Yu,[†] Chang-Sheng Wang,[‡] David B. Beach,[§] Yun-Dong Wu,*[,‡] and Zi-Ling Xue*[,†]

Contribution from the Department of Chemistry, The University of Tennessee, Knoxville, Tennessee 37996-1600, Department of Chemistry, The Hong Kong University of Science and Technology, Clear Water Bay, Kowloon, Hong Kong, China, and Chemical Sciences Division, Oak Ridge National Laboratory, Oak Ridge, Tennessee 37831-6197

Received December 22, 2004; E-mail: xue@utk.edu; chydwu@ust.hk

Abstract: Reactions of d^0 amides $M(NMe_2)_4$ (M = Zr, **1**; Hf, **2**) with O_2 have been found to yield unusual trinuclear oxo aminoxide complexes $M_3(NMe_2)_6(\mu\text{-}NMe_2)_3(\mu_3\text{-}O)(\mu_3\text{-}ONMe_2)$ (M = Zr, **3**; Hf, **4**) in high yields. Tetramethylhydrazine Me_2N-NMe_2 was also observed in the reaction mixtures. Crystal structures of **3** and **4** have been determined. Density functional theory calculations have been performed to explore the mechanistic pathways in the reactions of model complexes $Zr(NR_2)_4$ (R = H, **5**; Me, **1**) and $[Zr(NR_2)_4]_2$ (R = H, **5a**; Me, **1a**) with triplet O_2. Monomeric and dimeric reaction pathways in the formation of the Zr complex **3** are proposed.

Molecular approaches to thin films of metal oxides such as MO_2 (M = Ti, Zr, Hf) and Ta_2O_5 with large dielectric constants are of intense current interest.[1−3] These approaches are desired in part to yield new microelectronic insulating gate materials. The rapid developments in microelectronic technologies require continuous shrinking of device dimensions. In the new generations of ultra-large-scale-integration (ULSI) devices, the insulating gate layer needs to be less than 2 nm thick. At this thickness, SiO_2, the current insulating material with a low dielectric constant ($\kappa = 3.9$), is unacceptable,[1b] as its leakage current becomes large enough to be detrimental to the device operation. Thin films of metal oxides[1] with higher dielectric constants (e.g., ZrO_2, $\kappa = 25$) have been actively studied to replace SiO_2 as insulating gate materials to decrease the leakage current and maintain scaling.[1a] Reactions of d^0 amide complexes $M(NR_2)_n$ with O_2 have been actively studied to afford microelectronic metal oxide thin films.[2,3] The nature of these reactions and the mechanistic pathways leading to the formation of metal oxides are, however, not clear.

Reactions of transition metal complexes with O_2 are important in many biological and catalytic processes, and they have been of intense research interest.[4−6] Studies of these reactions with O_2 usually involve d^n transition metal complexes,[4−6] and the oxidation of metals often occurs in these reactions. There have been relatively few reports of reactions of d^0 metal complexes with O_2, and these reactions are mainly those of alkyl complexes.[7−18] Oxygen was found to insert into the Zr−alkyl bond in Cp_2ZrRCl forming $Cp_2Zr(OR)Cl$.[7] Reactions of Cp_2-

[†] The University of Tennessee.
[‡] The Hong Kong University of Science and Technology.
[§] Oak Ridge National Laboratory.

(1) (a) Wallace, R. M.; Wilk, G. D. *Crit. Rev. Solid State Mater. Sci.* **2003**, *28*, 231. (b) Smith, R. C.; Ma, T.; Hoilien, N.; Tsung, L. Y.; Bevan, M. J.; Colombo, L.; Roberts, J.; Campbell, S. A.; Gladfelter, W. L. *Adv. Mater. Opt. Electron.* **2000**, *10*, 105. (c) Kelly, P. V.; et al. *Adv. Mater. Opt. Electron.* **2000**, *10*, 115. (d) Senzaki, Y.; Hochberg, A. K.; Norman, J. A. T. *Adv. Mater. Opt. Electron.* **2000**, *10*, 93. (e) Lucovsky, G.; Phillips, J. C. *MRS Symp. Proc.* **1999**, *567* (*Ultrathin SiO_2 and High-κ Materials for ULSI Gate Dielectrics*), 201.
(2) (a) Bastianini, A.; Battiston, G. A.; Gerbasi, R.; Porchia, M.; Daolio, S. *J. Phys. IV* **1995**, *5*, C5−525. (b) Ohshita, Y.; Ogura, A.; Hoshino, A.; Hiiro, S.; Machida, H. *J. Cryst. Growth* **2001**, *233*, 292. (c) Hendrix, B. C.; Borovik, A. S.; Xu, C.; Roeder, J. F.; Baum, T. H.; Bevan, M. J.; Visokay, M. R.; Chambers, J. J.; Rotondaro, A. L. P.; Bu, H.; Colombo, L. *Appl. Phys. Lett.* **2002**, *80*, 2362. (d) Vaartstra, B. A. U.S. Patent 2004040501, 2004.
(3) Son, K.-A.; Mao, A. Y.; Sun, Y.-M.; Kim, B. Y.; Liu, F.; Kamath, A.; White, J. M.; Kwong, D. L.; Roberts, D. A.; Vrtis, R. N. *Appl. Phys. Lett.* **1998**, *72*, 1187.
(4) See, for example: (a) Feig, A. L.; Lippard, S. J. *Chem. Rev.* **1994**, *94*, 759. (b) Klotz, I. M.; Kurtz, D. M. *Chem. Rev.* **1994**, *94*, 567. (c) Theopold, K. H.; Reinaud, O. M.; Blanchard, S.; Leelasubeharoen, S.; Hess, A.; Thyagarajan, S. *ACS Symp. Ser.* **2002**, *823*, 75. (d) Kopp, D. A.; Lippard, S. J. *Curr. Opin. Chem. Biol.* **2002**, *6*, 568. (e) Que, L., Jr.; Tolman, W. B. *Angew. Chem., Int. Ed.* **2002**, *41*, 1114. (f) Brown, S. N.; Mayer, J. M. *Inorg. Chem.* **1992**, *31*, 4091. (g) Balch, A. L.; Cornman, C. R.; Olmstead, M. M. *J. Am. Chem. Soc.* **1990**, *112*, 2963.
(5) (a) Ezhova, M. B.; James, B. R. In *Advances in Catalytic Activation of Dioxygen by Metal Complexes*; Simándi, L. I., Ed.; Kluwer: Boston, 2003; Vol. 26, pp 1−77. (b) Zhang, C. X.; Liang, H.-C.; Humphreys, K. J.; Karlin, K. D. In *Advances in Catalytic Activation of Dioxygen by Metal Complexes*; Simándi, L. I., Ed.; Kluwer: Boston, 2003; Vol. 26, pp 79−121. (c) Funabiki, T. In *Advances in Catalytic Activation of Dioxygen by Metal Complexes*; Simándi, L. I., Ed.; Kluwer: Boston, 2003; Vol. 26, pp 157−226. (d) Boring, E.; Geletii, Y. V.; Hill, C. L. In *Advances in Catalytic Activation of Dioxygen by Metal Complexes*; Simándi, L. I., Ed.; Kluwer: Boston, 2003; Vol. 26, pp 227−264. (e) Simandi, L. I. In *Advances in Catalytic Activation of Dioxygen by Metal Complexes*; Simándi, L. I., Ed.; Kluwer: Boston, 2003; Vol. 26, pp 265−328.
(6) *The Activation of Dioxygen and Homogeneous Catalytic Oxidation*; Barton, D. H. R., Martell, A. E., Sawyer, D. T., Eds.; Plenum: New York, 1993.
(7) (a) Labinger, J. A.; Hart, D. W.; Seibert, W. E.; Schwartz, J. *J. Am. Chem. Soc.* **1975**, *97*, 3851. (b) Blackburn, T. F.; Labinger, J. A.; Schwartz, J. *Tetrahedron Lett.* **1975**, *16*, 3041.
(8) (a) Lubben, T. V.; Wolczanski, P. T. *J. Am. Chem. Soc.* **1985**, *107*, 701. (b) Lubben, T. V.; Wolczanski, P. T. *J. Am. Chem. Soc.* **1987**, *109*, 424.
(9) Brindley, P. B.; Scotton, M. J. *J. Chem. Soc., Perkin Trans. 2* **1981**, 419.
(10) Tilley, T. D. *Organometallics* **1985**, *4*, 1452.
(11) Wang, R.; Folting, K.; Huffman, J. C.; Chamberlain, L. R.; Rothwell, I. P. *Inorg. Chem. Acta* **1986**, *120*, 81.

 10.1021/ja042307u CCC: $30.25

ZrR_2 and $(tritox)_2MMe_2$ [M = Ti, Zr, Hf; tritox = $(Me_3C)_3$-CO] with O_2 give alkoxides $Cp_2Zr(OR)_2$ and $(tritox)_2M(OMe)_2$, respectively.[8,9] In the reaction of O_2 with $Cp_2Zr(SiMe_3)Cl$, O insertion into the Zr−Si bond was observed.[10] We recently found that the reaction of the silyl complex $(Me_2N)_4Ta-SiR_3$ with O_2 yielded O_2-stable $(Me_2N)_3Ta(\eta^2\text{-}ONMe_2)(OSiR_3)$.[17] When an equilibrium mixture of the silyl alkylidyne $(Bu^tCH_2)_2$-$W(\equiv CBu^t)(SiBu^tPh_2)$ and its bis(alkylidene) tautomer (Bu^tCH_2)-$W(=CHBu^t)_2(SiBu^tPh_2)$ was exposed to O_2, a migration of the silyl ligand to the alkylidyne ligand occurred yielding $(Bu^tCH_2)_2$-$W(=O)[=CBu^t(SiBu^tPh_2)]$.[18] Reactions of $M(NMe_2)_4$ (M = Zr, **1**; Hf, **2**) with O_2 have been investigated in an attempt to understand the nature of the reactions of d^0 amides with O_2 and the mechanistic pathways in the formation of metal oxides from the reactions. These reactions have been found to give trinuclear oxo aminoxy complexes $M_3(NMe_2)_6(\mu\text{-}NMe_2)_3$-$(\mu_3\text{-}O)(\mu_3\text{-}ONMe_2)$ (M = Zr, **3**; Hf, **4**). The formations of the oxo and aminoxy ligands here are rare in the reactions of d^0 complexes with O_2,[7−18] and they may be important steps in the removal of the amide ligands to give C-free oxides MO_2. Density functional theory (DFT) quantum mechanics calculations have been performed to understand the reaction between $Zr(NMe_2)_4$ (**1**) and O_2. Our preparation of trinuclear oxo aminoxy complexes $M_3(NMe_2)_6(\mu\text{-}NMe_2)_3(\mu_3\text{-}O)(\mu_3\text{-}ONMe_2)$ (**3**, **4**) and theoretical studies of the formation of the Zr complex **3** are presented.

Results and Discussion

Formation and Characterization of Trinuclear Oxo Aminoxy Complexes $M_3(NMe_2)_6(\mu\text{-}NMe_2)_3(\mu_3\text{-}O)(\mu_3\text{-}ONMe_2)$ (M = Zr, 3; Hf, 4). $Ti(NMe_2)_4$ in hexanes was found inert to O_2 at room temperature. Its other group 4 analogues $M(NMe_2)_4$ (M = Zr, **1**; Hf, **2**), however, readily reacted with O_2 at room temperature. Complexes **3** and **4** were prepared through the reactions of excess $M(NMe_2)_4$ (**1**, **2**) with O_2 in toluene or benzene and were isolated in 51.9% and 47.6% isolated yields (based on O_2), respectively. When monitored by ^1H NMR, the reaction of **1** with O_2 was found to yield **3** in ca. 87% yield. Analyses of volatiles that were removed in vacuo by GC−MS showed the presence of Me_2N-NMe_2. Reactions of **1** or **2** with O_2 in benzene-d_6 monitored by NMR also revealed the formation of Me_2N-NMe_2, and a small amount of $HNMe_2$. In the formation of **3**, the molar ratio of **3** to Me_2N-NMe_2 was at least 0.71, as determined by ^1H NMR. The step(s) to give the oxo ligands and tetramethylhydrazine is perhaps significant to yield metal oxides free of N and C impurities. Both complexes **3** and **4** are highly soluble in *n*-pentane, benzene, and toluene.

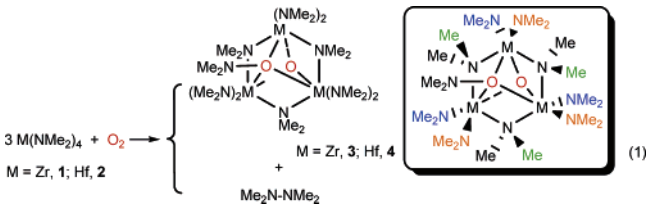

The ^1H and $^{13}C\{^1H\}$ NMR spectra of **3** and **4** are consistent with their structures. Assignments of the NMR resonances were confirmed by HMQC studies.[20] The resonances of the $ONMe_2$ ligand in **3** at 2.63 ppm in ^1H and 51.61 ppm in $^{13}C\{^1H\}$ NMR spectra are up- and downfield shifted, respectively, from those of the amide (NMe_2) ligands. Four other peaks were observed in both ^1H (in a 1:1:2:2 ratio) and $^{13}C\{^1H\}$ NMR spectra of **3**. The two 1:1 ^1H NMR peaks were assigned to the six methyl groups of the three bridging amide ligands: three above (green) and three below (black) the plane of the three Zr atoms (eq 1). Similarly, two 2:2 peaks were assigned to the terminal $-NMe_2$ ligands: three above (red) and three below (blue) the plane. Four peaks were also observed in the amide regions of the ^{13}C NMR spectrum of **3** at 23 °C. The observations of the four amide peaks suggest that the μ_3-bridging $O-NMe_2$ undergoes a fast rotation at room temperature, thus providing a pseudo C_3 symmetry in the complex. Similar NMR spectra were observed for the Hf analogue **4** at 23 °C. At −50 °C, the ^1H resonance of one set of the terminal $-NMe_2$ ligands in **4** split into two sets at 3.42 and 3.24 ppm, indicating restricted rotations along the Hf−N bonds for these ligands.[20] It is not clear why this occurs only with one of the two sets of the terminal $-NMe_2$ ligands in **4**, but not with its Zr analogue **3**.

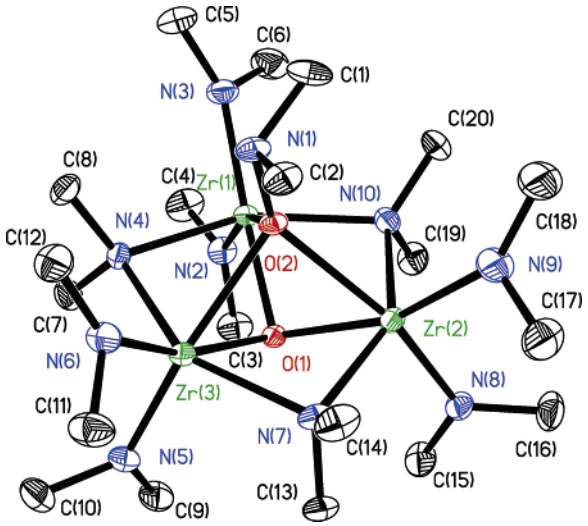

Figure 1. ORTEP view of **3** showing 30% probability thermal ellipsoids. The H atoms have been omitted for clarity. Selected bond distances (Å) and angles (deg): N(2)−Zr(1) 2.057(3), N(4)−Zr(1) 2.300(3), N(4)−Zr-(3) 2.291(3), O(1)−Zr(1) 2.119(2), O(2)−Zr(1) 2.415(2), N(1)−O(2) 1.469(3), Zr(3)−O(1)−Zr(1) 101.62(9), Zr(3)−O(2)−Zr(1) 85.76(7), N(1)−O(2)−Zr(2) 138.93(17), Zr(3)−N(4)−Zr(1) 91.28(9), N(4)−Zr(1)−N(10) 148.41(10), N(2)−Zr(1)−N(3) 100.70(13).

The molecular structures of complexes **3** and **4** are isomorphous, and their ORTEPs are shown in Figure 1 and the Supporting Information, respectively. Crystallographic data for **3** are given in Table 1.[20] The three Zr atoms and three bridging N atoms are essentially planar, forming a hexagon. The deviations of N(4), N(7), and N(10) from the plane defined by

(12) Gibson, V. C.; Redshaw, C.; Walker, G. L. P.; Howard, J. A. K.; Hoy, V. J.; Cole, J. M.; Kuzmina, L. G.; De Silva, D. S. *J. Chem. Soc., Dalton Trans.* **1999**, 161.
(13) Brindley, P. B.; Hodgson, J. C. *J. Organomet. Chem.* **1974**, *65*, 57.
(14) (a) Van Asselt, A.; Trimmer, M. S.; Healing, L. M.; Bercaw, J. E. *J. Am. Chem. Soc.* **1988**, *110*, 8254. (b) Coughlin, E. B.; Bercaw, J. E. *Organometallics* **1992**, *11*, 465.
(15) Gibson, T. *Organometallics* **1987**, *6*, 918.
(16) Kim, S.-J.; Jung, I. N.; Yoo, B. R.; Cho, S.; Ko, J.; Kim, S. H.; Kang, S. O. *Organometallics* **2001**, *20*, 1501.
(17) Wu, Z.-Z.; Cai, H.; Yu, X.-H.; Blanton, J. R.; Diminnie, J. B.; Pan, H.-J.; Xue, Z.-L. *Organometallics* **2002**, *21*, 3973.
(18) Chen, T.-N.; Wu, Z.-Z.; Li, L.-T.; Sorasaenee, K. R.; Diminnie, J. B.; Pan, H.-J.; Guzei, I. A.; Rheingold, A. L.; Xue, Z.-L. *J. Am. Chem. Soc.* **1998**, *120*, 13519. To our knowledge, this is the only other reported formation of an oxo ligand from the reaction of a d^0 complex(es) with O_2.
(19) Bradley, D. C.; Thomas, I. M. *J. Chem. Soc.* **1960**, 3857.
(20) See Supporting Information for details.

Table 1. Crystal Data and Structure Refinement for **3**

empirical formula (Fw)	$C_{20}H_{60}N_{10}O_2Zr_3$ (746.44)
temperature	−100(2) °C
crystal system and space group	orthorhombic, *Fdd*2
unit cell dimensions	$a = 25.767(10)$ Å, $\alpha = 90°$ $b = 28.493(17)$ Å, $\beta = 90°$ $c = 19.631(7)$ Å, $\gamma = 90°$
volume (calculated density)	14 413(12) Å^3 (1.376 g/cm^3)
Z	16
absorption coefficient	0.881 mm^{-1}
$F(000)$	6176
crystal size	0.65 × 0.53 × 0.45 mm^3
θ range for data collection	1.49−28.36°
index ranges	$-33 \le h \le 34$, $-37 \le k \le 37$, $-25 \le l \le 25$
reflections collected	33 464
independent reflections	8579 [R(int) = 0.0355]
completeness to $\theta = 28.36°$	97.2%
absorption correction	semiempirical from equivalents
max. and min. transmission	0.6925 and 0.5981
refinement method	full-matrix least-squares on F^2
data/restraints/parameters	8579/1/336
goodness-of-fit on F^2	0.855
final R indices [$I > 2\sigma(I)$][a]	R1 = 0.0275, wR2 = 0.0883
R indices (all data)	R1 = 0.0292, wR2 = 0.0907
absolute structure parameter	0.99(4)
largest diff. peak and hole	0.909 and −0.353 e Å^{-3}

[a] $R1 = \sum||F_o| - |F_c||/\sum|F_o|$; $wR2 = (\sum[w(F_o^2 - F_c^2)^2]/\sum[wF_o^2])^{1/2}$.

the Zr atoms are −0.1553, 0.0566, and 0.0352 Å, respectively. The average N−Zr−N and Zr−N−Zr angles are 148.91° and 90.89°, respectively. These Zr−μ_3-bridging-oxo bond distances [2.116(2)−2.119(2) Å] are, as expected, longer than those of the terminal Zr═O [1.804(4) Å in (η^5-$C_5Me_4Et)_2$Zr(═O)(Py)[21a]] and Zr−μ_2-oxo bonds [e.g., 1.94(1)−1.95(1) Å in $(Cp_2ZrO)_3$[21b]]. They agree with other Zr−μ_3-oxo bond distances.[21c] In contrast to the eight coordinated $Zr(ONMe_2)_4$ where the four β-N atoms donate their lone pair electrons to electron-deficient Zr atom,[22] the β-N atom in the dimethylaminoxy ligand −$ONMe_2$ in **3** does not coordinate to the Zr atoms.[23] The Zr−μ_3-O(2) bond distances of 2.409(2)−2.440(2) Å are significantly longer than those [2.054(2) and 2.102(1) Å] in $Zr(ONMe_2)_4$.[22] The average Zr−μ_3-oxo(1) bond distance of 2.118 Å for the double-bonded (═O) ligand in **3** is ca. 0.3 Å shorter than that (2.421 Å) for the single-bonded μ_3-O(2)−NMe_2 ligand. Zr−μ_3-oxo(1)−Zr bond angles of 101.62(9)−102.92(9)° in **3** are much larger than Zr−μ_3-O(2)−Zr bond angles of 85.44(6)−86.13(7)° for the aminoxy ligand.

The formations of both dimethylaminoxy −$ONMe_2$ and oxo ligands in **3** from the reaction of $Zr(NMe_2)_4$ (**1**) with O_2 in eq 1 are rare and worth noting.[7−18] The bridging μ_3-$ONMe_2$ ligand in **3** was formed through O insertion into a Zr−NMe_2 bond, although this formation may involve a multistep progress as theoretical studies (to be discussed below) suggest. In comparison, dialkylaminoxy complexes are usually prepared from the reactions of metal amides (or alkoxides) with hydroxylamine $HONR_2$ or reactions of metal halides with $LiONR_2$.[22,24] It is reasonable to assume that the $ONMe_2$ ligand is the precursor

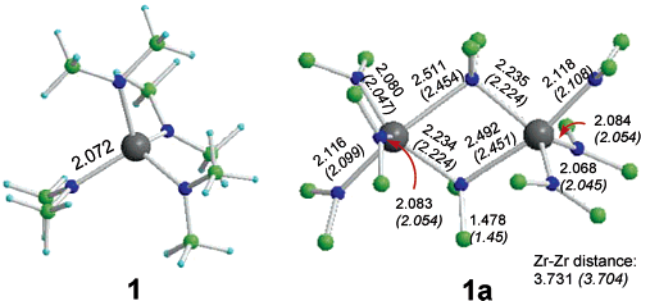

Figure 2. The calculated structures of $Zr(NMe_2)_4$ (**1**) and $[Zr(NMe_2)_4]_2$ (**1a**). The H atoms in **1a** are omitted for clarity. The calculated bond distances (Å) are compared to those in the crystal structure[29] (in parentheses).

to the oxo ligand in **3**. In other words, cleavage of the O−N bond in Zr−$ONMe_2$ leads to the formation of the μ_3-oxo ligand in **3**. The sequential steps here, that is, the initial formation of the aminoxy ligands and their subsequent conversion to oxo ligands, are important to the clean removal of the amide ligands and formation of C- and N-free metal oxides from metal amide precursors $M(NR_2)_n$.[2,3]

DFT Studies of the Reactions of O_2 with d^0 $Zr(NR_2)_4$ (R = H, 5; Me, 1). Reactions of O_2 with d^n transition metal complexes have been extensively investigated.[4−6] However, because conversions of electronic states are often involved in these reactions, theoretical studies in this field are limited. Over the past decade, blooming investigations of metalloenzymes and new developments in handling spin state conversions[26] have attracted many theoretical studies, both in the binding mode of O_2 with metal complexes[27] and in O_2 activation by metal complexes.[28] These studies have focused mainly on d^n transition metal complexes for their biological relevance. We are not aware of theoretical studies on reactions of d^0 transition metal complexes by O_2. In the current work, the mechanistic pathways in the reactions of O_2 with $Zr(NR_2)_4$ (R = H, **5**; Me, **1**) to give the trinuclear oxo aminoxy complex **3** have been investigated by DFT calculations.

$Zr(NMe_2)_4$ (**1**) exists as dimer $[Zr(NMe_2)_4]_2$ (**1a**) in the solid state,[29] and it is believed that there is an equilibrium between the monomer **1** and dimer **1a**.[29] To examine this equilibrium, the geometries of $Zr(NMe_2)_4$ (**1**) and $[Zr(NMe_2)_4]_2$ (**1a**) were optimized and shown in Figure 2. As in the crystal structure,[29] $[Zr(NMe_2)_4]_2$ (**1a**) is in a double-bridged manner. The optimized structure has a Zr−Zr distance of ca. 3.731 Å, only 0.026 Å

(21) (a) Howard, W. A.; Parkin, G. *J. Am. Chem. Soc.* **1994**, *116*, 606. (b) Fachinetti, G.; Floriani, C.; Chiesi-Villa, A.; Guastini, C. *J. Am. Chem. Soc.* **1979**, *101*, 1767. (c) Starikova, Z. A.; Turevskaya, E. P.; Kozlova, N. I.; Turova, N. Y.; Berdyev, D. V.; Yanovsky, A. I. *Polyhedron* **1999**, *18*, 941.
(22) Mitzel, N. W.; Parsons, S.; Blake, A. J.; Rankin, D. W. H. *J. Chem. Soc., Dalton Trans.* **1996**, 2089. For $Zr(ONEt_2)_4$, see: Wieghardt, K.; Tolksdorf, I.; Weiss, J.; Swiridoff, W. *Z. Anorg. Allg. Chem.* **1982**, *490*, 182.
(23) The terminal and bridging Zr−N bond distances in **3** are similar to those in other Zr amide complexes. See, for example: Wu, Z.-Z.; Diminnie, J. B.; Xue, Z.-L. *Inorg. Chem.* **1998**, *37*, 2570.
(24) (a) Singh, A.; Sharma, C. K.; Rai, A. K.; Gupta, V. D.; Mehrotra, R. C. *J. Chem. Soc. A* **1971**, 2440. (b) Lindemann, H. M.; Schneider, M.; Neumann, B.; Stammler, H.-G.; Stammler, A.; Jutzi, P. *Organometallics* **2002**, *21*, 3009. (c) Mitzel, N. W.; Vojinovic, K. *J. Chem. Soc., Dalton Trans.* **2002**, 2341.
(25) (a) Poli, R. *Acc. Chem. Res.* **1997**, *30*, 494. (b) Poli, R.; Harvey, J. N. *Chem. Soc. Rev.* **2003**, *32*, 1. (c) Harvey, J. N.; Poli, R.; Smith, K. M. *Coord. Chem. Res.* **2003**, *238*−*239*, 347.
(26) (a) Shaik, S.; Filatov, M.; Schröder, D.; Schwarz, H. *Chem.-Eur. J.* **1998**, *4*, 193. (b) Schröder, D.; Shaik, S.; Schwarz, H. *Acc. Chem. Res.* **2000**, *33*, 139.
(27) (a) Bytheway, I.; Hall, M. B. *Chem. Rev.* **1994**, *94*, 639. (b) Cramer, C. J.; Smith, B. A.; Tolman, W. B. *J. Am. Chem. Soc.* **1996**, *118*, 11283. (c) Eisenstein, O.; Getlicherman, H.; Giessner-Prettre, C.; Maddaluno, J. *Inorg. Chem.* **1997**, *36*, 3455. (d) Henson, N. J.; Hay, P. J.; Redondo, A. *Inorg. Chem.* **1999**, *38*, 1618. (e) Franzen, S. *Proc. Natl. Acad. Sci. U.S.A.* **2002**, *99*, 16754. (f) Jensen, K. P.; Ryde, U. *J. Biol. Chem.* **2004**, *279*, 14561.
(28) (a) Yoshizawa, K.; Ohta, T.; Yamabe, T.; Hoffmann, R. *J. Am. Chem. Soc.* **1997**, *119*, 12311. (b) Brunold, T. C.; Solomon, E. I. *J. Am. Chem. Soc.* **1999**, *121*, 8277. (c) Howe, P. R.; McGrady, J. E.; KcKenzie, C. J. *Inorg. Chem.* **2002**, *41*, 2026. (d) Wirstam, M.; Lippard, S. J.; Friesner, R. A. *J. Am. Chem. Soc.* **2003**, *125*, 3980. (e) Gherman, B. F.; Baik, M.-H.; Lippard, S. J.; Friesner, R. A. *J. Am. Chem. Soc.* **2004**, *126*, 2978.
(29) Chisholm, M. H.; Hammond, C. E.; Huffman, J. C. *Ployhedron* **1988**, *7*, 2515.

Scheme 1. The Energy Diagram of the Proposed Mechanism for the Formation of $Zr_3(NH_2)_6(\mu\text{-}NH_2)_3(\mu_3\text{-}O)(\mu_3\text{-}ONH_2)$ (**14**), a Model of **3**, from Mononuclear **5**[a]

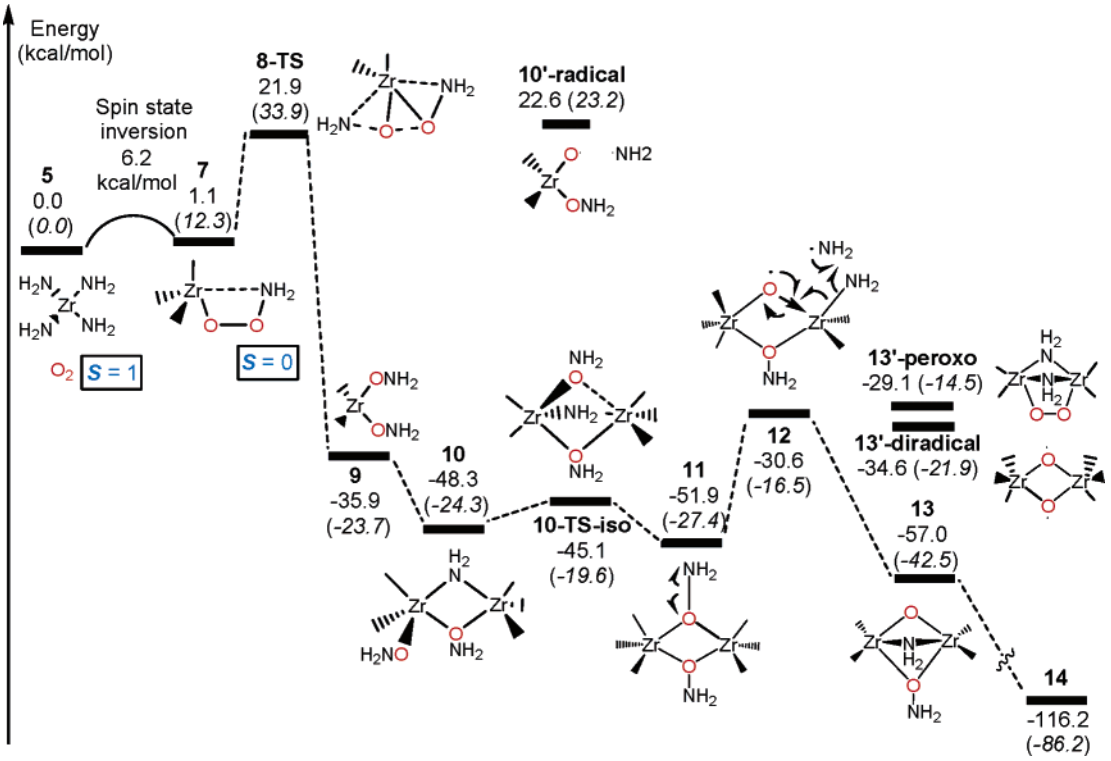

[a] The labels of some terminal NH_2's are omitted for clarity. The energies and free energies (in parentheses) are in kcal/mol.

Chart 1

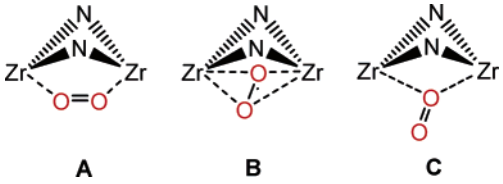

longer than that in the crystal structure.[29] The calculated Zr−N bond distances (Figure 2), both in the terminal and in the bridge, are close to those in the crystal structure of **1a**.[29] This suggests that the B3LYP method is good at reproducing the real structures. The calculated complexation energy of the dimer is only ca. 0.5 kcal/mol. Although more accurate methods are needed to obtain better energetics, the current calculations indeed indicate that both the monomer and the dimer may be the active species.

We next investigated how triplet O_2 binds to $Zr(NMe_2)_4$ (**1**) and $[Zr(NMe_2)_4]_2$ (**1a**). For the tetrahedron monomer, no complex associated with triplet O_2 could be located. For the dimer (**1a**), at least three binding modes (Chart 1) are possible. Neither the side-on mode (**B**) nor the single end-on mode (**C**) could be obtained in the optimization. The end-on mode **A**, as shown in **6** in Figure 3, was found to be more stable than the separated $Zr(NMe_2)_4$ dimer (**1a**) and O_2 by ca. 9.8 kcal/mol based on single-point energy calculations with the basis set II on the geometries obtained with the basis set I. This indicates that such a binding process is exothermic. Although the binding of O_2 is nearly symmetrical with the two Zr−O distances of 2.298 and 2.328 Å, respectively, one of the bridging NMe_2 shifts toward Zr(1) so that the two Zr centers become unsymmetrical. This shift might be a result of electron transfer from NMe_2

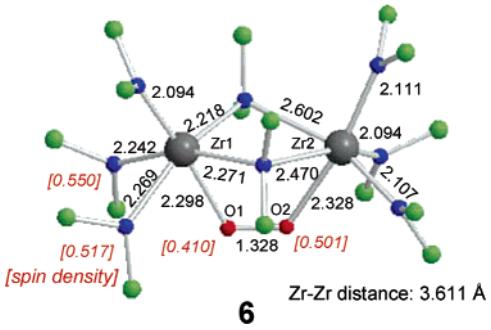

Figure 3. The calculated structure of $[Zr(NMe_2)_4]_2$ (**1a**)−triplet O_2 complex (**6**) with spin densities (in parentheses). The H atoms are omitted for clarity. The bond distances are in angstroms.

ligand to O_2. As shown in Figure 3, the spin densities are not only localized on the two O atoms, but are also shared by two N atoms attached to Zr(1), resulting in two slightly elongated Zr(1)−N bonds. As a result, the Zr(1) center becomes electron poorer and has a stronger tendency to draw electrons from the bridging NMe_2, resulting in shorter Zr(1)−N(bridging) distances.

Reactions of O_2 with Monomers $Zr(NR_2)_4$ (R = H, 5; Me, 1). Calculations for the detailed pathways for the reactions of $Zr(NMe_2)_4$ (**1**) and $[Zr(NMe_2)_4]_2$ (**1a**) with O_2 to form the trinuclear oxo aminoxy complex **3** would be too costly. We calculated detailed reaction pathways between the reactions of $Zr(NH_2)_4$ (**5**) and $[Zr(NH_2)_4]_2$ (**5a**) with O_2. This allowed us to carry out the calculations at a high level, as discussed in computational details in Experimental Section. Because the reaction occurs at the metal centers, we reasoned that the replacement of NMe_2 by NH_2 may not cause a significant difference.[30] The proposed monomeric mechanistic pathway is shown in Scheme 1, and the optimized structures are given in Figure 4.

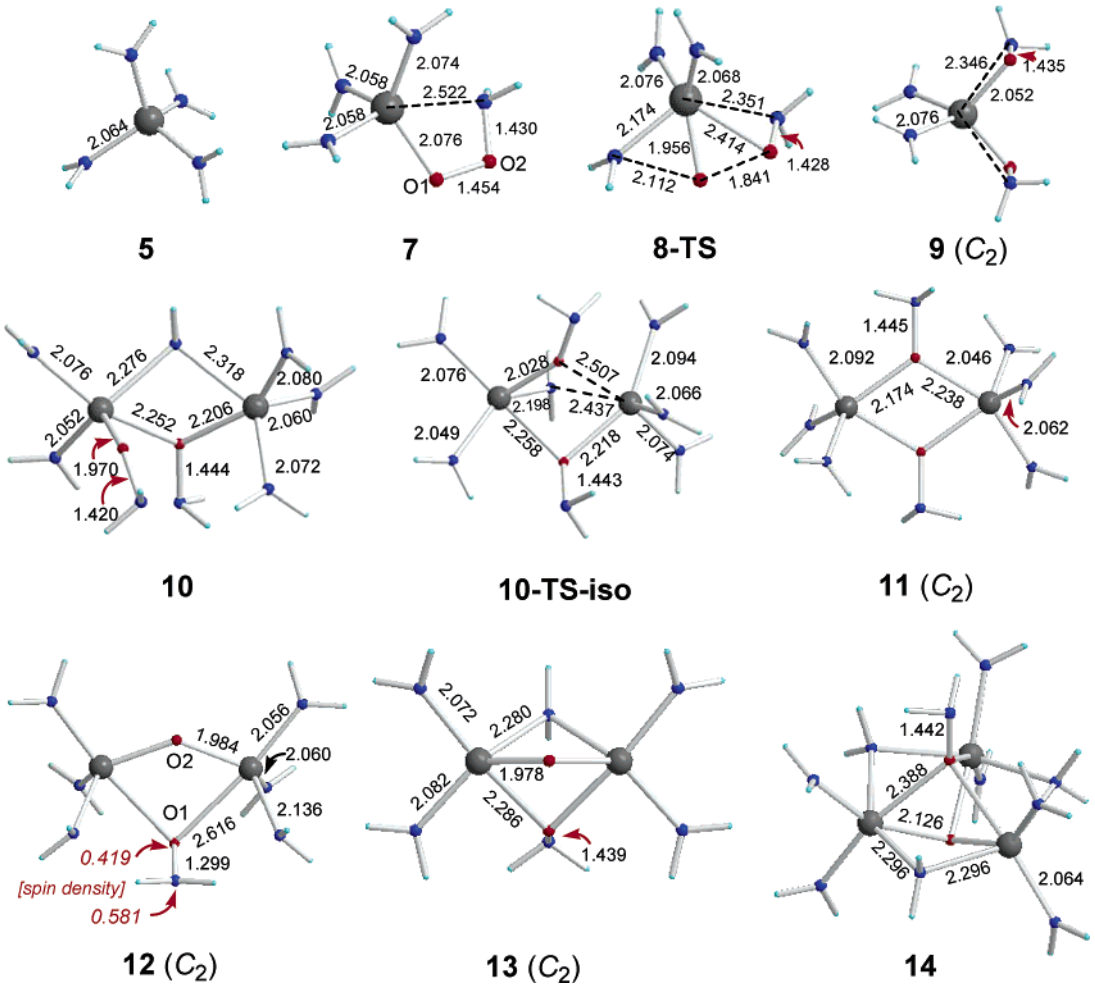

Figure 4. Optimized geometries of the proposed complexes in Scheme 1. Bond distances are in angstroms.

Because the attempts to locate the complex between triplet O_2 and monomer $Zr(NH_2)_4$ (**5**) failed, the sum of the energies of the isolated triplet O_2 and $Zr(NH_2)_4$ (**5**) was set as the reference energy level. The singlet adduct between O_2 and $Zr(NH_2)_4$ (**5**) is a peroxo complex $Zr(NH_2)_3(O-ONH_2)$ (**7**). This process involves O_2 spin-crossing from the triplet ground state to singlet. We were unable to locate a transition structure for such a spin-crossing process because multireference calculations would be necessary, which is prohibitively expensive for the current system. Extensive efforts have been taken to find the minimum-energy-crossing-point (MECP) to estimate the activation energy for the spin-crossing process.[25b] Three separated sets of calculations were carried out, using O(1)−O(2), Zr−N, and O(1)−Zr distances as the reaction coordinate, respectively. The geometries were optimized in the triplet and singlet states, respectively, by constraining the reaction coordinate at different values. Interestingly, the three individual sets of calculations all give the energy of the MECP to be ca. 6.2 kcal/mol higher than the reactants.[20] This indicates that the oxygen insertion into the Zr−N bond in **5** to form **7** has a low activation barrier. **7** is, however, an unstable intermediate, and the calculated reaction free energy is ca. 12.3 kcal/mol. The symmetric $Zr(NH_2)_2(ONH_2)_2$ (**9**) is generated from peroxo complex $Zr(NH_2)_3(O-ONH_2)$ (**7**) via an O−O bond cleavage transition structure (**8-TS**). The calculated activation free energy is ca. 33.9 kcal/mol with respect to the reactants. Homolytic N−O bond cleavage in $Zr(NH_2)_2(ONH_2)_2$ (**9**) results in a very unstable complex $ZrO(NH_2)_2(ONH_2)\bullet$ (**10′-radical**) with a relative energy of 22.6 kcal/mol. The calculated N−O bond dissociation energy (BDE) of ca. 58.4 kcal/mol is close to that of a normal N−O bond. This indicates that N−O homolytic bond cleavage in mononuclear **9** is unlikely. Combining $Zr(NH_2)_2(ONH_2)_2$ (**9**) with $Zr(NH_2)_4$ (**5**) yields the dinuclear complex $(H_2N)_2(H_2NO)Zr(\mu\text{-}NH_2)(\mu\text{-}ONH_2)Zr(NH_2)_3$ (**10**). **10** can be easily isomerized into C_2 symmetrical $(H_2N)_3Zr(\mu\text{-}ONH_2)_2Zr(NH_2)_3$ (**11**), which is more stable than **10** by ca. 4.1 kcal/mol, through a low barrier transition state **10-TS-iso**. A concerted transition structure for H_2N-NH_2 elimination from **11** to give **13** directly could not be located. Instead, a homolytic N−O bond cleavage of **11** to yield $\bullet[(H_2N)_3Zr(\mu\text{-}O)(\mu\text{-}ONH_2)Zr(NH_2)_3]$ radical (**12**) (Scheme 1) and $\bullet NH_2$ radical was found to be fairly favorable. Due to a spin delocalization stabilization, the N−O BDE (21.3 kcal/mol) in the dinuclear complex (**11**) is significantly lower than that in the mononuclear complex (**9**) (58.4 kcal/ mol). In the C_{2v} symmetrical structure **12**, the spin density is mainly located in the O(1)−N moiety, resulting in a remarkable increase in the Zr−O(1) distance (2.616 Å) (Figure 4). The Zr−O(2) distance

(30) (a) Liu, X.-Z.; Wu, Z.-Z.; Peng, Z.-H.; Wu, Y.-D.; Xue, Z.-L. *J. Am. Chem. Soc.* **1999**, *121*, 5350. (b) Xue, Z.-L.; et al. *J. Am. Chem. Soc.* **2001**, *123*, 8011. (c) Wu, Y.-D.; Peng, Z.-H.; Chan, K. W. K.; Liu, X.-Z.; Tuinman, A. A.; Xue, Z.-L. *Organometallics* **1999**, *18*, 2081.

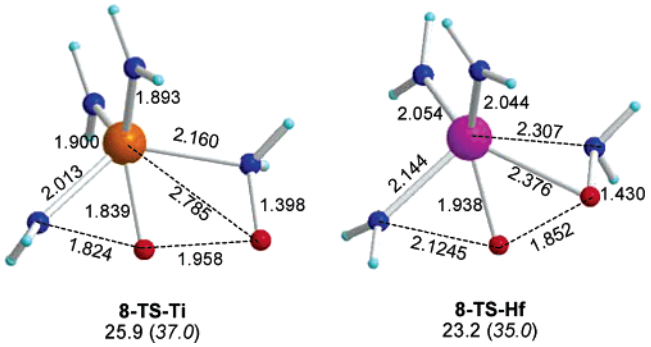

Figure 5. The optimized geometries of **8-TS-Ti** and **8-TS-Hf** for the reactions of $Ti(NH_2)_4$ and $Hf(NH_2)_4$ with O_2. The bond distances are in angstroms. The calculated relative energies and relative free energies (in parentheses) with respect to the isolated reactants are in kcal/mol.

is 1.984 Å in **12**, representing a Zr−μ_2-oxo bond.[22] After the N−O bond dissociation, the reactive •NH_2 radical can abstract a NH_2 group either from O−NH_2 or from Zr−NH_2 to form H_2N-NH_2. If NH_2 abstraction is from the O−NH_2 bridge, a tri-bridged peroxo complex **13′-peroxo** or a diradical complex **13′-diradical** shall form. The calculated reaction energies of the two processes are ca. 1.5 and −4.0 kcal/mol, respectively. On the other hand, NH_2 abstraction from Zr−NH_2 to form $(H_2N)_2Zr(\mu\text{-}O)(\mu\text{-}ONH_2)(\mu\text{-}NH_2)Zr(NH_2)_2$ (**13**, Scheme 1) and H_2N-NH_2 is very exothermic (by ca. 27 kcal/mol). Structure **13** is found to be more stable than **13′-peroxo** and **13′-diradical** by over 20 kcal/mol. Therefore, the NH_2 abstraction from Zr−NH_2 should be much more favorable than that from the O−NH_2 bridge. The easy homolytic O−N bond cleavage (in **11**) and favorable •NR_2 radical abstraction not only explain the formation of Me_2N-NMe_2 in the experiment, but are also in agreement with the observation of a small amount of $HNMe_2$ as a byproduct. By capping with one more molecule of $Zr(NH_2)_4$ (**5**) on its vacant side, **13** turns into the final product $Zr_3(NH_2)_6(\mu\text{-}NH_2)_3(\mu_3\text{-}O)(\mu_3\text{-}ONH_2)$ (**14**), which is consistent with the crystal structure of **3**. The calculated Zr−μ_3-oxo and Zr−μ_3-O(2)NMe_2 bond distances are ca. 2.13 and 2.38 Å, respectively. The average terminal and bridging Zr−N bond distances are ca. 2.08 and 2.29 Å, respectively. As compared to the Zr−N bond distances of 2.057(3), 2.291(3), and 2.300(3) Å in the X-ray structure of **3**, the discrepancies are with 0.03 Å. The reaction is exothermic with an overall reaction free energy of −86.2 kcal/mol.

The rate-determining transition structure is **8-TS** with an activation free energy of ca. 33.9 kcal/mol. The counterparts of **8-TS** for the reactions of $Ti(NH_2)_4$ and $Hf(NH_2)_4$ with O_2 were also located. These structures, which are given in Figure 5, have geometrical features similar to those of structure **8-TS**. The calculated activation free energies with **8-TS-Ti** and **8-TS-Hf** are ca. 37.0 and 35.0 kcal/mol, respectively, somewhat higher than that with **8-TS** (33.9 kcal/mol). Although these calculated high activation free energies in the gas phase are somewhat overestimated for solution reactions,[32] it appears that the experimentally observed formation of **3** and **4** from the reactions of $Zr(NMe_2)_4$ and $Hf(NMe_2)_4$ with O_2 at room temperature is difficult to explain by this monomeric reaction mechanism.

The Reaction of O_2 with Dimer $[Zr(NH_2)_4]_2$ (5a). To make comparisons, the sum of the energies of $Zr(NH_2)_4$ (**5**) and O_2, which was the reference energy level in the monomeric pathway, was set as the reference in the dimeric pathway as well.[33] The reliability of replacing NMe_2 ligand by NH_2 was examined with the calculated structure of triplet complex **15** (Figure 6) formed between $[Zr(NH_2)_4]_2$ (**5a**) and triplex O_2. Indeed, **15** maintained the geometric parameters of its NMe_2 analogue **6** (Figure 3). The calculated relative energy of **15** with respect to the reactants is ca. −13.0 kcal/mol, similar to that of **6** with respect to the corresponding reactants. This indicates that the approach of using $Zr(NH_2)_4$ as a model for $Zr(NMe_2)_4$ is reasonable.

Starting from this triplet complex **15**, a proposed mechanism based on calculation results is shown in Scheme 2. The geometries of the calculated intermediates, transition structures, and the product are shown in Figure 6.

Upon changing the spin state of **15** from triplet to singlet, an intermediate **16** yielded from the insertion of O(1) to one of the Zr(1)−N bonds. This singlet intermediate **16** (Scheme 2 and Figure 6) is slightly more stable than the triplet intermediate **15**. Interestingly, the singlet complex **16** is not as symmetric as we expected. The O(1)−N(2) bond (1.464 Å) is formed with both the O(1) and the N atoms weakly coordinated to Zr(1). The O(1)−O(2) bond distance is increased to 1.464 Å, indicating a normal O−O single bond. It is noted that the insertion reaction should be accompanied by a spin-crossing, which was not studied. However, the barrier of this process is likely low based on the calculations for the similar process in the reaction of $Zr(NH_2)_4$ with O_2 (Scheme 1). The intermediate **16** undergoes NH_2 migration from Zr(2) to O(2) to break the O(1)−O(2) bond. This transition structure is early with the newly formed N(3)---O(2) distance of ca. 2.20 Å, while the O(1)−O(2) distance elongates to ca. 1.69 Å. The reaction has an activation free energy of ca. 8.8 kcal/mol (8.3 kcal/mol in terms of activation energy). Because the transition structure **17-TS** is reactant-like, an internal reaction coordinate (IRC) calculation was carried out, which indicates that **17-TS** leads to the formation of a stable intermediate **10**. The thermodynamic driving force (ΔG) for this step of reaction (**16** → **10**) is ca. −35.9 kcal/mol. **10** then follows the same pathway (through **11**, **12**, and **13**) as shown in Scheme 1 to generate the final product **14**. Therefore, the rate-determining step in the dimeric pathway in Scheme 2 is the intramolecular O−O bond cleavage (**17-TS**), which has an activation free energy of 19.6 kcal/mol. This barrier is much lower than that in the monomeric mechanism in Scheme 1. This indicates that the dimeric mechanism in Scheme 2 is viable under the experimental conditions.

The key difference between the monomeric and dimeric mechanisms is in the reactivity of the O−O bond cleavage, which is the rate-determining step. In the dimeric mechanism, the dioxygen coordinates with two metal centers and the O−O

(31) Bradley, D. C.; Thomas, I. M. *Proc. Chem. Soc.* **1959**, 225.
(32) This is a bimolecular reaction. The calculated loss of entropy in the gas phase is overestimated as compared to a solution reaction. Therefore, the calculated activation free energy is somewhat overestimated.

(33) Unlike the crystal and calculated double-bridged structures of $[Zr(NMe_2)_4]_2$ (**1a**), the optimized $[Zr(NH_2)_4]_2$ (**5a**) is a tri-bridged dimer with the Zr−Zr distance of 3.295 Å. The replacement of NMe_2 by NH_2 reduces the steric effect in the bridging region and thus makes such a dimer preferred. Therefore, $[Zr(NH_2)_4]_2$ (**5a**), which cannot properly represent the real system, was ignored in further discussion. A question was whether NH_2 ligands could represent NMe_2 ligands in other species. After reexamining the calculated structures, we believe that the steric problem as a result of replacing NMe_2 by NH_2 is only significant for bridging amide ligands in $[Zr(NH_2)_4]_2$ (**5a**) for its short Zr−Zr distance. Other structures bear much less effect. That is proven by the comparison of the geometries of **6** and **15**.

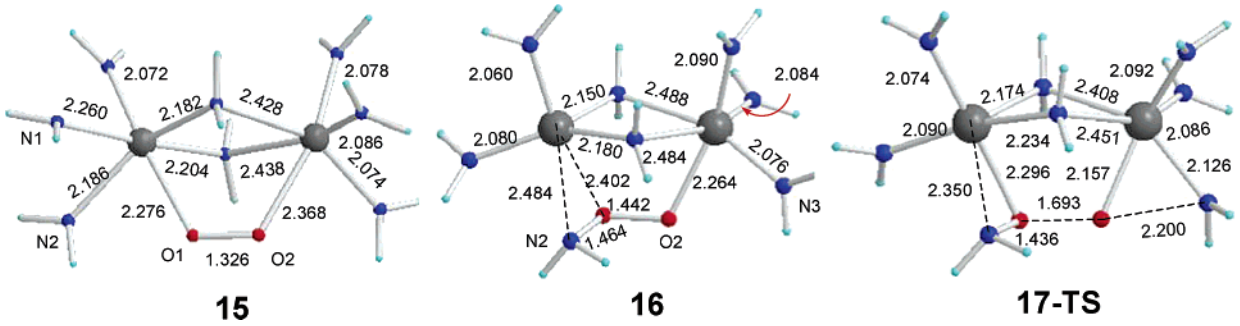

Figure 6. The optimized geometries of the proposed complexes in Scheme 2. The bond distances are in angstroms.

Scheme 2. The Energy Diagram of the Proposed Dimeric Mechanism for the Formation of Trinuclear Zr Complex **14**[a]

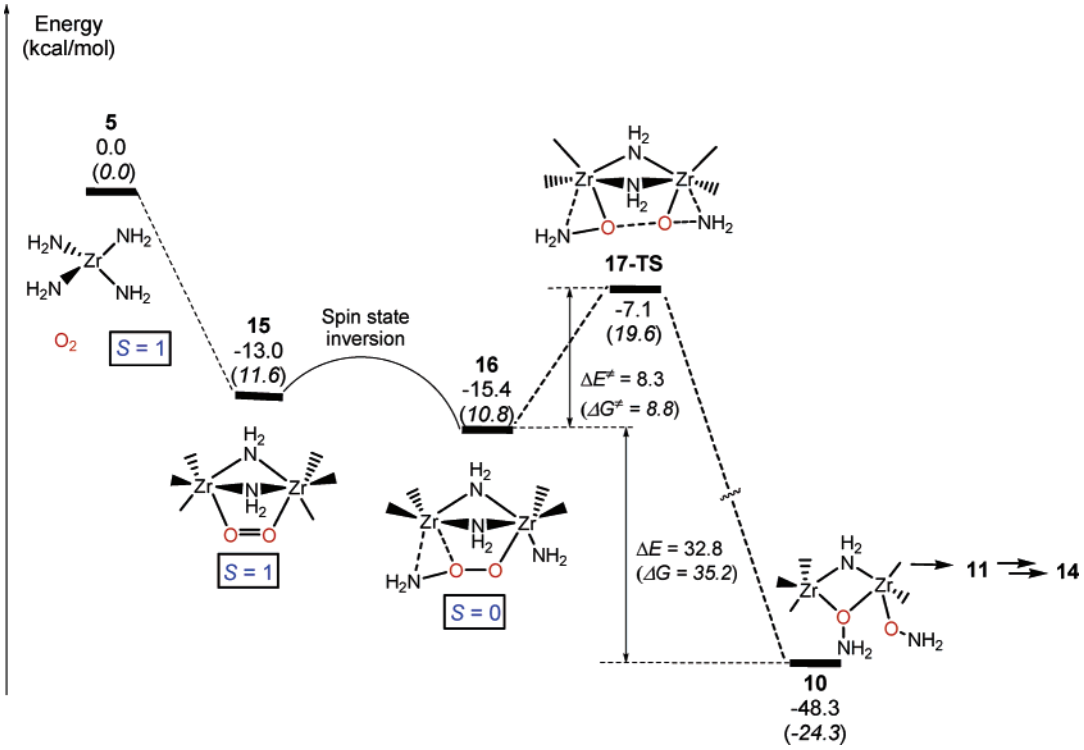

[a] Some terminal NH_2 groups are omitted for clarity. The energies and free energies (in parentheses) are in kcal/mol.

bond is more activated. The calculated free energy difference between **17-TS** and **16** is only ca. 8.8 kcal/mol. On the other hand, in the monomeric mechanism (Scheme 1), the leaving O(2) group in **8-TS** cannot gain sufficient stabilization, and the calculated free energy difference between **8-TS** and **7** is ca. 21.6 kcal/mol. Therefore, the dimeric mechanism is more favorable than the monomeric pathway when the reaction is carried out in solution and at low temperature. This implies that the existence of (μ-NMe_2) dinuclear complex might be important to the formation of the $M_3(NMe_2)_6(\mu\text{-}NMe_2)_3(\mu_3\text{-}O)(\mu_3\text{-}ONMe_2)$ (M = Zr, **3**; Hf, **4**). For Zr and Hf, the (μ-NR_2)-bridged complexes are reported frequently.[29,30b,34] On the other hand, because Ti is smaller than Zr and Hf, dimerization of titanium amide complexes with (μ-NR_2) bridges becomes more difficult.[35] This might explain why $Ti(NMe_2)_4$ is inert to O_2 at room temperature.

Concluding Remarks

The formation of oxo aminoxy complexes $M_3(NMe_2)_6(\mu\text{-}NMe_2)_3(\mu_3\text{-}O)(\mu_3\text{-}ONMe_2)$ (M = Zr, **3**; Hf, **4**) suggests two important steps in the reactions of $M(NMe_2)_4$ (M = Zr, **1**; Hf, **2**) with diradical O_2: (a) oxygen insertion into M−N bonds leading to the formation of aminoxy ligands; and (b) cleavage of the O−N bond in the aminoxy O−NMe_2 ligands to yield the oxo ligands in **3**, **4**. These two steps to give the rarely observed formations of the ligands[7−18] are perhaps among the elementary steps in the clean formation of metal oxides free of C and N contamination from the reactions of d^0 metal amides with O_2.

Both monomeric and dimeric mechanistic pathways for the formation of $M_3(NMe_2)_6(\mu\text{-}NMe_2)_3(\mu_3\text{-}O)(\mu_3\text{-}ONMe_2)$ (M = Zr, **3**; Hf, **4**) have been proposed on the basis of quantum mechanical calculations for the model reactions of triplet O_2

(34) (a) Danièle, S.; Hitchcock, P. B.; Lappert, M. F.; Merle, P. G. *Dalton Trans.* **2001**, 13. (b) O'Connor, P. E.; Berg, D. J.; Barclay, T. *Organometallics* **2002**, *21*, 3947. (c) Lehn, J.-S. M.; Hoffman, D. M. *Inorg. Chem.* **2002**, *41*, 4063. (d) Passarelli, V.; Benetollo, F.; Zanella, P.; Carta, G.; Rossetto, G. *Dalton Trans.* **2003**, 1411.

(35) We only find two examples of dimeric titanium amide complexes. In these cases, the amide ligands are either tetradentate or tridentate so that steric interactions are reduced: (a) Olmstead, M. M.; Power, P. P.; Viggiano, M. *J. Am. Chem. Soc.* **1983**, *105*, 2927. (b) Fredrich, S.; Gade, L. H.; Edwards, A. I.; McPartlin, M. *Chem. Ber.* **1993**, *126*, 1797.

with $Zr(NR_2)_4$ (R = H, **5**; Me, **1**). The results indicate that triplet O_2 can easily insert into $Zr(NH_2)_4$ (**5**) or $[Zr(NH_2)_4]_2$ (**5a**) via spin-crossing. This is followed by rate-determining NH_2 migration to O with O−O bond cleavage. It is found that the dimeric reaction is more kinetically favorable than the monomeric reaction. Both reactions then give intermediate $(H_2N)_3Zr(\mu\text{-}ONH_2)_2Zr(NH_2)_3$ (**11**), which undergoes a homolytic O−NH_2 cleavage to give oxo radical intermediate $\bullet[(H_2N)_3Zr(\mu\text{-}O)(\mu\text{-}ONH_2)Zr(NH_2)_3]$ (**12**) and $\bullet NH_2$. Abstraction of $\bullet NH_2$ from Zr center by $\bullet NH_2$ and addition of $Zr(NH_2)_4$ (**5**) yield H_2N-NH_2 and trinuclear complex **14**. The dimeric pathway has a much lower activation energy than the monomeric pathway at room temperature.

Experimental Section

General Procedures. All manipulations were performed under a dry and oxygen-free nitrogen atmosphere with the use of glovebox or Schlenk techniques. Solvents were purified by refluxed in and distilled from potassium/benzophenone ketyl. Benzene-d_6 and toluene-d_8 were dried and stored over activated molecular sieves under nitrogen. $M(NMe_2)_4$ (M = Zr, **1**;[19,29] Hf, **2**[19]) was prepared according to the literature methods. NMR spectra were recorded on a Bruker AMX-400 Fourier transform spectrometer. A Hewlett-Packard 6890 gas chromatograph (GC) with a 5973 mass selective detector (MSD) was used to obtain GC/MS data. Elemental analyses were conducted by Complete Analysis Laboratories Inc., Parsippany, NJ.

Preparation of $Zr_3(NMe_2)_6(\mu\text{-}NMe_2)_3(\mu_3\text{-}O)(\mu_3\text{-}ONMe_2)$ (3). $Zr(NMe_2)_4$ (**1**, 1.00 g, 3.71 mmol) in toluene (10 mL) was cooled with liquid nitrogen and pumped for 10 min to remove nitrogen gas. The mixture was then warmed to room temperature, and 0.412 mmol of O_2 was added through a gas manifold. The solution was stirred overnight. All volatiles were removed in vacuo, leaving a white solid. The excess $Zr(NMe_2)_4$ (**1**) was removed from this solid in vacuo at room temperature. The residues were then extracted with *n*-pentane, and the filtrate was concentrated and cooled to −32 °C to afford colorless crystals of **3** (0.160 g, 0.214 mmol, 51.9% yield based on O_2). ^{1}H NMR (benzene-d_6, 400.18 MHz, 23 °C): δ 3.21 (s, 18H, 3N*Me*$_{2-a}$), 2.98 (s, 18H, 3N*Me*$_{2-b}$), 2.89 (s, 9H, 3μ-N*Me*$_c$Me$_d$), 2.85 (s, 9H, 3μ-NMe$_c$*Me*$_d$), 2.63 (s, 6H, ON*Me*$_2$). ^{13}C NMR (benzene-d_6, 100.63 MHz, 23 °C): δ 51.74 (ON*Me*$_2$), 46.32 (μ-NMe$_c$*Me*$_d$), 45.79 (N*Me*$_{2-a}$), 45.56 (μ-N*Me*$_c$-Me$_d$), 42.52 (N*Me*$_{2-b}$). Anal. Calcd for $C_{20}H_{60}N_{10}O_2Zr_3\cdot{}^1/_4C_5H_{12}$: C, 33.39; H, 8.31. Found: C, 33.19; H, 8.17.

Preparation of $Hf_3(NMe_2)_6(\mu\text{-}NMe_2)_3(\mu_3\text{-}O)(\mu_3\text{-}ONMe_2)$ (4). $Hf(NMe_2)_4$ (**2**, 1.00 g, 2.82 mmol) in toluene (10 mL) was cooled with liquid nitrogen and pumped for 10 min to remove nitrogen gas. The mixture was warmed to room temperature, and 0.412 mmol of O_2 was added. The solution was stirred overnight. Volatiles and the excess $Hf(NMe_2)_4$ (**2**) were removed in vacuo at room temperature. The residue was then extracted with *n*-pentane, and the filtrate was cooled to −32 °C to give colorless crystals of **4** (0.198 g, 0.196 mmol, 47.6% yield based on O_2). ^{1}H NMR (benzene-d_6, 400.18 MHz, 23 °C): δ 3.26 (s, 18H, 3N*Me*$_{2-a}$), 3.02 (s, 18H, 3N*Me*$_{2-b}$), 2.94 (s, 9H, 3μ-N*Me*$_c$Me$_d$), 2.84 (s, 9H, 3μ-NMe$_c$*Me*$_d$), 2.66 (s, 6H, ON*Me*$_2$). ^{13}C NMR (benzene-d_6, 100.63 MHz, 23 °C): δ 51.61 (ON*Me*$_2$), 45.63 (N*Me*$_{2-a}$; μ-NMe$_c$-*Me*$_d$), 45.13 (μ-N*Me*$_c$Me$_d$), 43.11 (N*Me*$_{2-b}$). ^{1}H NMR (toluene-d_8, 400.18 MHz, 23 °C): δ 3.23 (s, 18H, 3N*Me*$_{2-a}$), 3.01 (s, 18H, 3N*Me*$_{2-b}$), 2.94 (s, 9H, 3μ-N*Me*$_c$Me$_d$), 2.83 (s, 9H, 3μ-NMe$_c$*Me*$_d$), 2.68 (s, 6H, ON*Me*$_2$). ^{13}C NMR (toluene-d_8, 100.63 MHz, 23 °C): δ 51.66 (ON*Me*$_2$), 45.63 (N*Me*$_{2-a}$; μ-NMe$_c$*Me*$_d$), 45.21 (μ-N*Me*$_c$Me$_d$), 43.15 (N*Me*$_{2-b}$). ^{1}H NMR (toluene-d_8, 400.18 MHz, −60 °C): δ 3.42 (s, 9H, 3N*Me*$_a$Me$_{a'}$), 3.24 (s, 9H, 3NMe$_a$*Me*$_{a'}$), 3.05 (s, 18H, 3N*Me*$_{2-b}$), 2.92 (s, 9H, 3μ-N*Me*$_c$Me$_d$), 2.87 (s, 9H, 3μ-NMe$_c$*Me*$_d$), 2.59 (s, 6H, ON*Me*$_2$). ^{13}C NMR (toluene-d_8, 100.63 MHz, −60 °C): δ 51.76 (ON*Me*$_2$), 46.86 (N*Me*$_a$Me$_{a'}$), 45.76 (μ-NMe$_c$*Me*$_d$), 45.05 (μ-N*Me*$_c$Me$_d$), 44.76 (NMe$_a$*Me*$_{a'}$), 43.10 (N*Me*$_{2-b}$). Anal. Calcd for $C_{20}H_{60}N_{10}O_2Hf_3\cdot{}^1/_2C_5H_{12}$: C, 25.88; H, 6.37. Found: C, 25.74; H, 6.25.

X-ray Crystal Structure Determination of 3 and 4. A crystal of **3** or **4** was selected in Paratone oil and mounted on a hairloop. The data were collected on a Bruker AXS Smart 1000 X-ray diffractometer (Mo Kα radiation, 0.71073 Å) with a CCD area detector under a N_2 stream at −100(2) °C. The structures were solved by direct methods. Non-H atoms were refined with anisotropic coefficients, and all H atoms were treated as idealized contributions. An empirical correction was performed with SADABS.[36a] In addition, the global refinements for the unit cells and data reductions of the two structures were performed using the Saint program (Version 6.02). All calculations were performed using the SHELXTL (Version 5.1) proprietary software package.[36b]

Computational Details. All calculations were performed using the Gaussian 03 package[37] with density functional theory at the B3LYP level. Basis sets that allowed a meaningful description of the system were chosen. Different basis sets are chosen for the different systems to balance the accuracy and the computational cost. For the complex with the realistic ligand NMe_2, full geometric optimizations and vibration frequency calculations were carried out with basis set I: LanL2DZ with f polarization functions for Zr, 6-31+G* for core part elements N and O, and 3-21G for the C and H in the methyl groups. For the complex with the simplified ligand NH_2, basis set II: LanL2DZ with f polarization functions for Zr, Ti, and Hf, and the 6-31+G* basis set for all of the other elements, were employed. The calculated relative energies shown in the text have been corrected with zero-point energy (ZPE).

Acknowledgment. We acknowledge the National Science Foundation (CHE-0212137), Research Grants Council of Hong Kong (HKUST6087/02P), Department of Energy, and Ziegler Research Fund for financial support of this research.

Supporting Information Available: Complete refs 1c and 30b, a molecular view of **4**, 2D HMQC NMR spectra of **3** at 23 °C and **4** at −50 °C, crystallographic data for **3** and **4**, and search for spin-crossing and coordinates of calculated structures. This material is available free of charge via the Internet at http://pubs.acs.org.

JA042307U

(36) (a) Sheldrick, G. M. *SADABS, A Program for Empirical Absorption Correction of Area Detector Data*; University of Göttingen: Göttingen, Germany, 2000. (b) Sheldrick, G. M. *SHELXL-97, A Program for the Refinement of Crystal Structures*; University of Göttingen: Göttingen, Germany, 1997.

(37) Frisch, M. J.; Trucks, G. W.; Schlegel, H. B.; Scuseria, G. E.; Robb, M. A.; Cheeseman, J. R.; Montgomery, J. A., Jr.; Vreven, T.; Kudin, K. N.; Burant, J. C.; Millam, J. M.; Iyengar, S. S.; Tomasi, J.; Barone, V.; Mennucci, B.; Cossi, M.; Scalmani, G.; Rega, N.; Petersson, G. A.; Nakatsuji, H.; Hada, M.; Ehara, M.; Toyota, K.; Fukuda, R.; Hasegawa, J.; Ishida, M.; Nakajima, T.; Honda, Y.; Kitao, O.; Nakai, H.; Klene, M.; Li, X.; Knox, J. E.; Hratchian, H. P.; Cross, J. B.; Adamo, C.; Jaramillo, J.; Gomperts, R.; Stratmann, R. E.; Yazyev, O.; Austin, A. J.; Cammi, R.; Pomelli, C.; Ochterski, J. W.; Ayala, P. Y.; Morokuma, K.; Voth, G. A.; Salvador, P.; Dannenberg, J. J.; Zakrzewski, V. G.; Dapprich, S.; Daniels, A. D.; Strain, M. C.; Farkas, O.; Malick, D. K.; Rabuck, A. D.; Raghavachari, K.; Foresman, J. B.; Ortiz, J. V.; Cui, Q.; Baboul, A. G.; Clifford, S.; Cioslowski, J.; Stefanov, B. B.; Liu, G.; Liashenko, A.; Piskorz, P.; Komaromi, I.; Martin, R. L.; Fox, D. J.; Keith, T.; Al-Laham, M. A.; Peng, C. Y.; Nanayakkara, A.; Challacombe, M.; Gill, P. M. W.; Johnson, B.; Chen, W.; Wong, M. W.; Gonzalez, C.; Pople, J. A. *Gaussian 03*, revision B.03; Gaussian, Inc.: Pittsburgh, PA, 2003.